CSIRO

Convective mixing in geological storage of CO$_2$

Christopher P. Green and Jonathan Ennis-King
Report Number EP13096
February 1, 2013

Copyright and disclaimer

Important disclaimer

Acknowledgement

Contents

Abstract

Numerical simulations are an essential tool for assessing the long-term storage of CO_2 in saline aquifers, such as the pilot project at the Wandoan site in Queensland's Surat Basin. However, the robustness of the numerical predictions is dependent on accurately capturing the essential physical processes involved. One of the most significant results obtained through numerical simulations is the partitioning of CO_2 into immobile phases, particularly the amount immobilised at residual saturation and the amount that has dissolved into the resident formation water. The quantity and time scale for CO_2 immobilised in this manner is critical for understanding the security of the geological storage, as it reduces the possibility of leakage into shallower formations.

It is well known that the necessary use of large grid blocks in numerical simulations of field-size projects introduces errors in the predictions of the amount of dissolved CO_2. Recent work has provided simple solutions to correct this error (Green and Ennis-King, 2012). Another consequence of large grid blocks that has not yet been adequately addressed is the failure to accurately include the effects of convective mixing. This fine-scale process, which acts to increase the dissolution rate of CO_2 into the formation water, has been the subject of a large body of scientific literature in recent years. Unfortunately, methods to include this effect in field-scale simulations, such as those that will be required for storage in the Precipice Sandstone in the Surat (e.g. the Wandoan site), are lacking.

In this report, a review of the current body of knowledge concerning convective mixing of CO_2 in saline aquifers is presented, and plans for future research to address the present shortcomings are detailed.

1 Introduction

Geological storage of carbon dioxide as a means to reduce anthropomorphic emission of greenhouse gases is one of the possible strategies currently being explored. It is the subject of a very large body of scientific research worldwide, with a corresponding large body of published literature.

One of the most likely storage options is sequestration in deep saline aquifers (van der Meer, 1992; Bachu et al., 1994), where CO_2 is injected into the resident formation brine. Storage security can be achieved through several mechanisms. The most commonly considered storage mechanism is structural trapping, where an impermeable caprock forms a structural closure that prevents buoyant migration of injected CO_2 beyond the caprock.

In the case where CO_2 is injected into a saline aquifer with a bounding cap rock, buoyancy drives vertical migration of the mobile CO_2 (CO_2 in the supercritical gas phase), which then spreads beneath the cap rock to form a thin, laterally extensive plume of gas phase CO_2, see Figure 1.1. In time, the gaseous CO_2 begins to dissolve into the local formation water, leading to a small increase in density of the saturated brine at the top of the aquifer. Diffusion of the dissolved CO_2 allows further dissolution, a process that leads to a gravitational instability whereby a denser fluid lies atop a less dense one. This process is known as convection, where motion is induced as vertical acceleration overcomes diffusion. Weir et al. (1996) first observed the formation of a convection cell during numerical simulations of CO_2 storage in a deep saline aquifer.

An example of the onset of convection and the subsequent formation of downwelling fingers of dissolved CO_2 obtained from high resolution numerical simulations by Pau et al. (2010) is presented in Figure 1.2. In this figure, we can observe the formation of small, regular perturbations in the dissolved CO_2 concentration, which grow and form fingers.

Shortly after Weir et al. (1996), Lindeberg and Wessel-Berg (1997) explicitly considered both temperature and density-driven convection of a plume of CO_2 lying atop brine. Using a simplified approach based on well-known methods for analysing temperature-driven convection in porous media, they presented a basic stability criteria for the onset of convection. Lindeberg and Wessel-Berg (1997) noted that convection could drive the dissolution rate faster than diffusion alone, making it an important
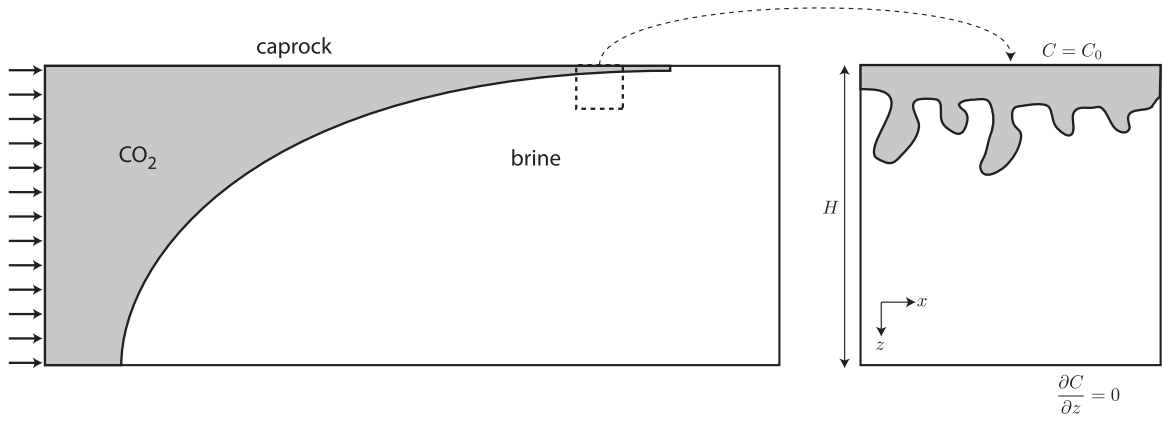
Figure 1.1: Schematic of the CO_2 injection in a horizontal reservoir bounded by an impermeable caprock. The shaded region represents CO_2 in the mobile (supercritical) gas phase, which migrates upwards and spreads beneath the caprock. The close up view of the dashed box shows the commonly used model for studies of the convective mixing process.

mechanism for the safe storage of CO_2 in geological formations.

Fine-scale numerical studies by Lindeberg and Bergmo (2003), Ennis-King and Paterson (2003), and Ennis-King and Paterson (2005) verified the presence of convection, with the now-familiar fingers of CO_2 saturated brine sinking deep into the unsaturated brine modelled in detail numerically, and observed experimentally. These studies demonstrated that the rate of dissolution of gaseous CO_2 into the formation brine accelerates sharply at the onset of convective mixing, suggesting that convective mixing has an important role in the safe long-term storage of CO_2 in saline aquifers.

A significant body of scientific literature concerned with understanding the convective mixing process in the storage of CO_2 in saline aquifers followed in the ensuing years, with research spanning theoretical analysis, numerical simulations and experimental validations. This review article presents an overview of this research effort and suggests some directions for future research.

2 Governing equations

Convective mixing of dissolved CO_2 in brine is a complex problem described by coupled differential equations. The equations governing this density-driven convective mixing are Darcy's law for fluid flow in a porous media, and the convection-diffusion equation for transport of the dissolved solute. They are commonly expressed as

$$\mathbf{u} = -\frac{k}{\mu}\left(\nabla P - \rho_f g \hat{z}\right), \tag{2.1}$$

and

$$\phi\frac{\partial C}{\partial t} + \mathbf{u} \cdot \nabla C = \phi D \nabla^2 C, \tag{2.2}$$

where $\mathbf{u}$ is the Darcy velocity, k is permeability, μ is the fluid viscosity, P is the pressure, ρ_f is the fluid density, g is the acceleration due to gravity, $\hat{z}$ is the unit vector in the direction of gravity, ϕ is the porosity of the porous medium, C is the solute concentration, t is time, and D is the diffusion coefficient, the product of diffusivity and tortuosity (Ennis-King et al., 2005). The fluid is also assumed to be incompressible, so
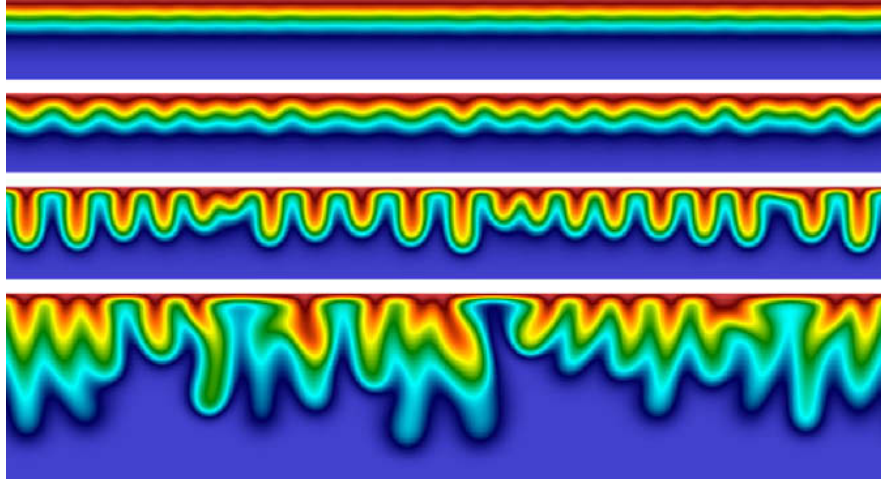
$$\nabla \cdot \mathbf{u} = 0. \tag{2.3}$$

Figure 1.2: Evolution of density-driven convection of CO_2 concentration in the liquid phase (dissolved CO_2). Time increasing from top to bottom. Figure from Pau et al. (2010).

The coupling between Eqs. (2.1) and (2.2) arises due to the effect on fluid density of the concentration of solute, which is given by

$$\rho_f = \rho_0 \left(1 + \frac{\Delta\rho}{\rho_0 C_0} C \right), \tag{2.4}$$

where ρ_0 is the density of the unsaturated fluid, C_0 is the maximum solute concentration, and $\Delta\rho = \rho - \rho_0$ is the maximum density increase with concentration. In the following, it will be assumed that $\Delta\rho > 0$, i.e., that increased solute concentration increases fluid density. This assumption is appropriate for dissolved CO_2.

To simplify the analysis, it is commonly assumed that the dependence of ρ_f on C is only retained in the buoyancy term in Eq. (2.1), effectively linearising the dependence of density to concentration. This approximation, known as the Boussinesq approximation (Bear, 1972), is appropriate for CO_2 dissolved in brine due to the weak dependence of partial molar volume on concentration (Ennis-King et al., 2005).

The governing equations are completed with appropriate boundary and initial conditions. If the porous media is considered an infinitely long horizontal reservoir of fixed height H, see Figure 1.1, the boundary conditions at the top ($z = 0$) and bottom ($z = H$) surfaces are given by

$$w(x, 0, t) = 0, \qquad w(x, H, t) = 0, \tag{2.5}$$

$$C(x, 0, t) = C_0, \qquad \left. \frac{\partial C(x, z, t)}{\partial z} \right|_{z=H} = 0, \tag{2.6}$$

respectively, where C_0 is the solubility of CO_2 in brine. The physical significance of these boundary conditions are to represent a fixed concentration at the upper surface, and a no-flux boundary at the base of the reservoir. The presence of a fixed concentration boundary at the upper surface is supported by the numerical simulation studies of Lindeberg and Bergmo (2003), Ennis-King and Paterson (2003), and Ennis-King and Paterson (2005), where it was observed that the interface between the gaseous CO_2 and brine remains sharp despite the presence of fingers of CO_2 saturated brine sinking into the less dense unsaturated brine. In reality, this assumption is a simplification of the true interface at the boundary layer, where two phase flow exists.

The initial conditions are

$$\mathbf{u}(x, z, 0) = 0, \qquad C(x, z, 0) = 0 \text{ for } z > 0, \tag{2.7}$$

which correspond to no initial velocity and zero initial solute concentration in the reservoir (apart from the top boundary).

Significant insight into the importance of various processes and properties can be obtained by non-dimensionalising the governing equations. For the case of the horizontal reservoir considered in Figure 1.1, several choices of scaling are obvious. Concentration C is scaled by C_0, and all lengths are scaled by the reservoir height H. Typical diffusive scales are employed for time and velocity. Velocities are therefore scaled by $\phi D / H$, and time is scaled by H^2/D. Pressure is scaled by $\phi \mu D / k$. The governing equations, boundary conditions and initial conditions become

$$\mathbf{u}^* = -\nabla P^* + Ra C^* \hat{z}, \tag{2.8}$$

$$\frac{\partial C^*}{\partial t^*} + \mathbf{u}^* \cdot \nabla C^* = \nabla^2 C^*, \tag{2.9}$$

$$w^*(x^*, 0, t^*) = 0, \qquad w^*(x^*, 1, t^*) = 0, \tag{2.10}$$

$$C^*(x^*, 0, t^*) = 1, \qquad \left.\frac{\partial C^*(x^*, z^*, t^*)}{\partial z^*}\right|_{z^*=1} = 0, \tag{2.11}$$

$$\mathbf{u}^*(x^*, z^*, 0) = 0, \qquad C^*(x^*, z^*, 0) = 0 \text{ for } z^* > 0, \tag{2.12}$$

where the superscript asterisk denotes a dimensionless variable, and Ra is the Rayleigh number, given by

$$Ra = \frac{k \Delta \rho g C_0 H}{\phi \mu D}. \tag{2.13}$$

This dimensionless number is a measure of the relative importance of density-driven convection to purely diffusive motion. When Ra is large, convection may occur.

3 Homogeneous media

Due to the coupled nature of the equations governing convective mixing in a porous medium, analytical results are limited to a small number of tractable cases featuring simplistic models. The vast majority of these cases concern homogeneous reservoirs.

Most theoretical studies have focussed on estimating the critical time for the onset of convective mixing, the critical wavelength of the fingers that form as the dense CO_2 rich brine mixes into the less dense unsaturated brine, and the rate of mass transfer of CO_2 due to convective mixing. A detailed review of the instability of boundary layers in porous media is presented in Rees et al. (2008), where results from different approaches are compared and evaluated. In most cases, only linear systems are considered.

Ennis-King and Paterson (2003), and Ennis-King and Paterson (2005) used linear stability analysis to estimate the critical time for the onset of convective mixing, t_c, given by

$$t_c = c_1 \frac{\phi^2 \mu^2 D}{k^2 (\Delta \rho)^2 g^2}, \tag{3.1}$$

where c_1 is a constant. Ennis-King and Paterson (2005) calculated $c_1 \approx 78$ for an isotropic, homogenous porous media. Using a similar analysis, Xu et al. (2006) calculated $c_1 = 75.19$.

Riaz et al. (2006) used a different time scale in their analysis of this problem, scaling time with $\phi H^2/D$, and consequently obtained slightly different results for the critical time and the value of
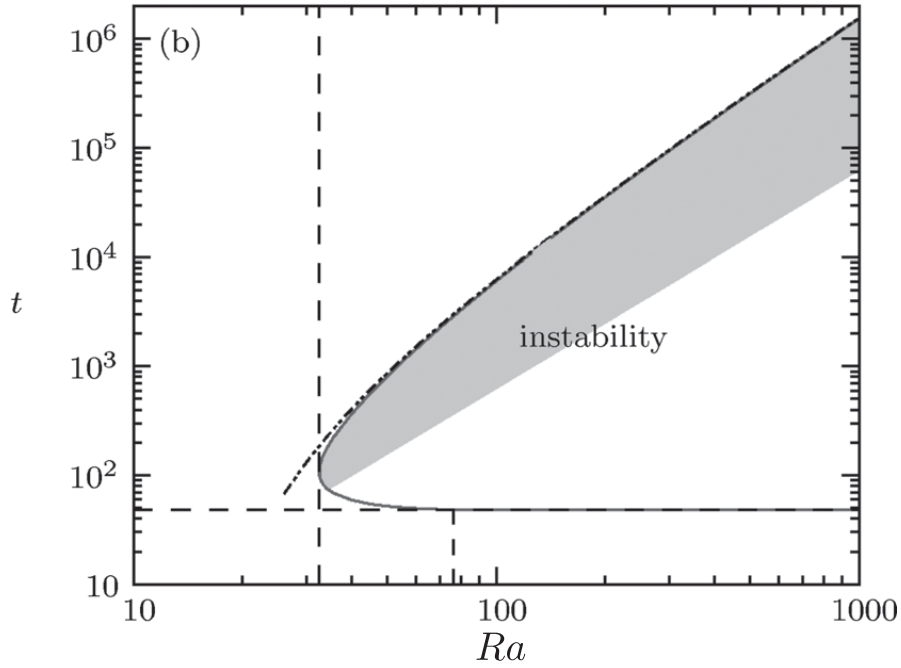
Figure 3.1: Instability region for convective mixing in a homogenous porous medium. For $Ra < 32.5$, no convection is possible. For $Ra > 75$, onset time is independent of Ra. Figure from Slim and Ramakrishnan (2010).

the constant. A detailed numerical study by Pau et al. (2010) demonstrated that the choice of scale presented in this article is more appropriate for this problem. Specifically, Pau et al. (2010) demonstrated that t_c varies linearly with ϕ^2 and D, while being inversely proportional to k, and thus verified the functional form of Eq. (3.1).

Slim and Ramakrishnan (2010) extended the theoretical analysis of the critical time for the onset of density-driven convection in a porous medium using linear stability and energy stability techniques. In so doing, they derived critical times for various regimes of Ra. Unlike previous studies that relied on implicit assumptions of when a perturbation occurs, no such assumptions are necessary. Slim and Ramakrishnan (2010) present stability diagrams showing that no convection is possible for $Ra < 32.5$, see Figure 3.1. Above this value of the Rayleigh number, convection is possible with a minimum onset time depending on Ra. For $Ra > 75$, the earliest possible time for the onset of a convective instability is independent of Ra, and is given by Eq. (3.1) but with a constant given by $c_1 = 47.9$. This time is significantly earlier than that estimated by Ennis-King and Paterson (2005) and Xu et al. (2006).

The critical wavelength λ_c of the instability is then (Ennis-King and Paterson, 2005; Xu et al., 2006)

$$\lambda_c = c_2 \frac{\phi \mu D}{k \Delta \rho g}, \tag{3.2}$$

where c_2 is a constant. Ennis-King and Paterson (2005) calculates $c_2 \approx 92$, while Xu et al. (2006) gives a value of $c_2 = 96.23$.

These expressions for the critical time and critical wavelength were extended to the case of anisotropic homogenous media by Ennis-King and Paterson (2005) and Ennis-King et al. (2005). When anisotropy is included, the constants c_1 and c_2 become functions of the ratio of vertical to horizontal permeability $\gamma = k_v/k_h$, where k_v and k_h are the permeabilities in the vertical and horizontal directions,
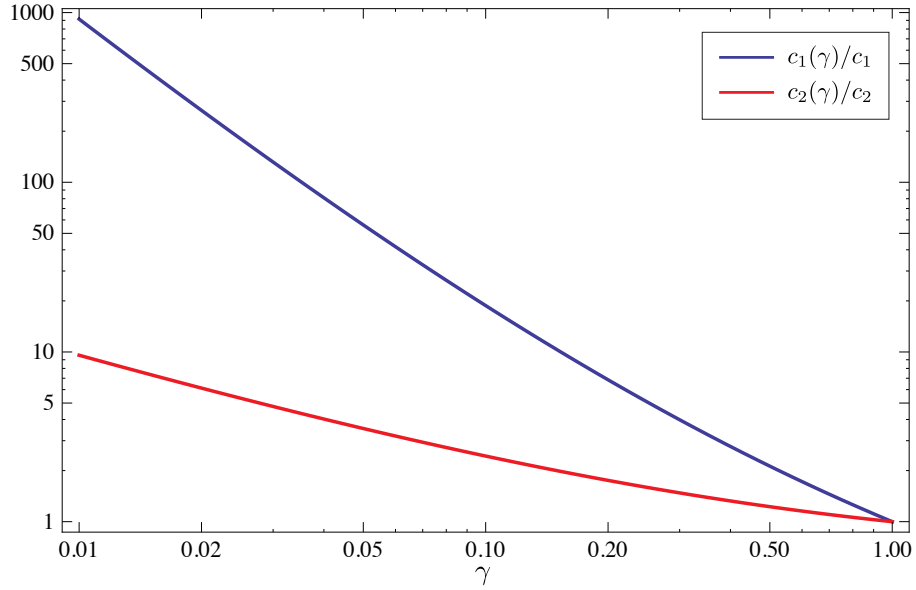
Figure 3.2: Effect of anisotropy $\gamma = k_v/k_h$ on the critical time parameter $c_1(\gamma)$ and the critical wavelength parameter $c_2(\gamma)$.

respectively. The functional form of these coefficients are given by (Ennis-King and Paterson, 2005; Ennis-King et al., 2005)

$$c_1(\gamma) \approx c_1 \frac{\left(1 + \sqrt{\gamma}\right)^4}{16\gamma^2}, \tag{3.3}$$

$$c_2(\gamma) \sim c_2 \frac{\left(1 + \sqrt{\gamma}\right)^2}{4\gamma^{3/4}}. \tag{3.4}$$

Figure 3.2 demonstrates the effect of permeability anisotropy on the critical time for the onset of convection, as well as the critical wavelength of the fingers. It is evident that reducing the vertical permeability in comparison to the horizontal permeability has a dramatic effect on the time for the onset of the convective instability, while having only a small effect on the wavelength of the fingers.

High resolution numerical simulations have shown that the mass flux oscillates about a constant value in the long term, with temporal variations of the order of 15% (Hesse et al., 2006; Pruess and Zhang, 2008; Pau et al., 2010), see Figure 3.3 . The functional form of this long-term mass flux of CO_2 per unit width in a two-dimensional model, F_m, is given by (Hesse et al., 2006; Pau et al., 2010)

$$F_m \approx 0.017 \frac{kC_0\Delta\rho g}{\mu}, \tag{3.5}$$

where the constant 0.017 is calculated from numerical results.

Pau et al. (2010) also presented analogous results for three dimensions, observing that the mass flux exhibits similar long-term behaviour as the two-dimensional case.

Neufeld et al. (2010) examined the relationship between the convective mass flux and Ra, and determined through numerical simulations and experimental analogues that the convective mass flux scales as $Ra^{4/5}$, in contrast with the classical linear relationship. Using simple analytical arguments, Neufeld et al. (2010) provided a theoretical basis for their findings findings. However, the dependence on the reservoir height suggests that this finding is valid for a regime where the downward flux of CO_2 is influenced by the base of the reservoir.
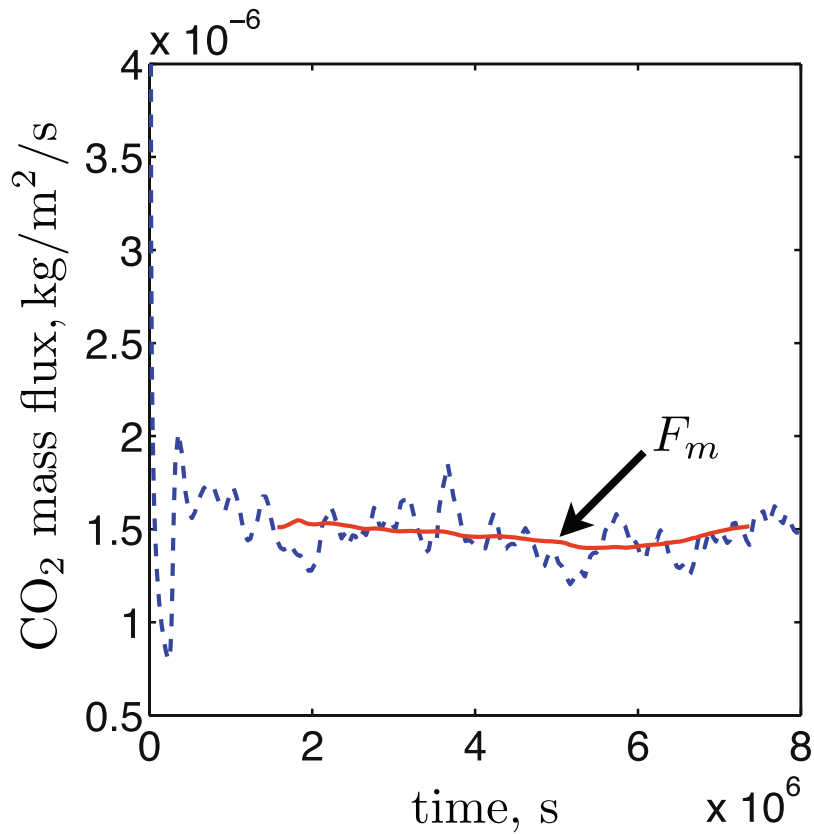
Figure 3.3: CO_2 mass flux as a function of time. The long-term mass flux F_m is indicated. Figure from Pau et al. (2010).

Elenius and Johannsen (2012) investigated the onset time of the fully nonlinear convective regime, defined by the authors as the time where the dissolution rate shows a rapid increase from the initial diffusive decay. This rapid increase corresponds to the point in time where the convective fingers begin to coalesce. Note that this time is different to the critical time for the onset of convection t_c discussed earlier. Ensemble averages of 300 simulations with various initial perturbations are used to examine the time for the onset of the fully nonlinear regime, where it was observed that this time was more than 30 times larger than t_c. This finding suggests that the onset time for fully nonlinear convection should be used in practical applications to field-scale simulations.

Typical values for the critical time for the onset of convection, t_c, the critical wavelength λ_c, and the long-term mass flux of CO_2 due to convective mixing for typical reservoir parameters are presented in Table 3.2. Typical fluid properties are given in Table 3.1.

In these examples, convective mixing can occur at times ranging from less than one year up to over one hundred years, depending on permeability and porosity. The critical wavelength ranges from tens of metres to tens of centimetres, and the long-term steady mass flux varies from 1.4×10^{-9} kg m^{-2} s^{-1} to 144×10^{-9} kg m^{-2} s^{-1}.

These values suggest that convective mixing occurs relatively quickly in comparison to the total simulated life of a project, which may be thousands of years. Importantly, the critical wavelength, which can be on the cm scale, is typically orders of magnitude smaller than the lateral dimensions

Table 3.1: Typical fluid properties.

Viscosity, μ	0.5947×10^{-3} (kg m^{-1} s^{-1})
Unsaturated brine density, ρ_0	994 (kg m^{-3})
Saturated brine density, ρ	1004.5 (kg m^{-3})
CO_2 solubility in brine, C_0	49.0 (kg m^{-3})
Diffusion coefficient, D	2×10^{-9} (m^2 s^{-1})

Table 3.2: Critical time for the onset of convection t_c, critical wavelength λ_c, and long-term mass flux F_m. Typical fluid properties presented in Table 3.1.

ϕ	k (md)	t_c (s)	λ_c (m)	F_c (kg m^{-2} s^{-1})
	10	5.2×10^8	10.7	1.4×10^{-9}
0.1	100	5.2×10^6	1.1	14.4×10^{-9}
	1000	5.2×10^4	0.1	144.4×10^{-9}
	10	2.1×10^9	21.3	1.4×10^{-9}
0.2	100	2.1×10^7	2.1	14.4×10^{-9}
	1000	2.1×10^5	0.2	144.4×10^{-9}
	10	4.7×10^9	32.0	1.4×10^{-9}
0.3	100	4.7×10^7	3.2	14.4×10^{-9}
	1000	4.7×10^5	0.3	144.4×10^{-9}

of numerical grid blocks used in field-scale simulations. As a result, field-scale simulations do not properly account for the increased dissolution rate due to convective mixing.

4   Heterogeneous media

In contrast to homogeneous reservoirs, comparatively little work on understanding convective mixing in heterogeneous porous media is present in the literature. In particular, theoretical estimates of useful quantities such as the critical time for the onset of convection, the critical wavelength and even the critical value of Ra are lacking. Only a limited number of numerical studies of the effects of heterogeneity on the characteristics of convection have been undertaken, with these providing few broadly applicable observations.

Some inspiration for theoretical analysis may possibly be drawn from studies concerning thermal convection in heterogeneous porous media (Nield and Simmons, 2006; Nield and Kuznetsov, 2007; Nield and Simmons, 2007; Simmons et al., 2010). For example, Nield and Simmons (2007) presented an approximate criterion for the establishment of convection in a heterogeneous porous medium.

Studies involving reservoir heterogeneity are usually limited to a simplified but representative form of heterogeneity. One model of heterogeneity that has been applied in practice is a simple model containing thin, horizontal flow barriers in a homogenous medium. This simple formulation is relatively simple to implement in numerical simulations, and provides a reservoir where the vertical permeability is significantly smaller than the horizontal permeability, as is often observed in actual reservoirs.

Green and Ennis-King (2009) presented detailed numerical simulations of convective mixing in a porous medium containing a random distribution of lateral flow barriers in an otherwise homogenous
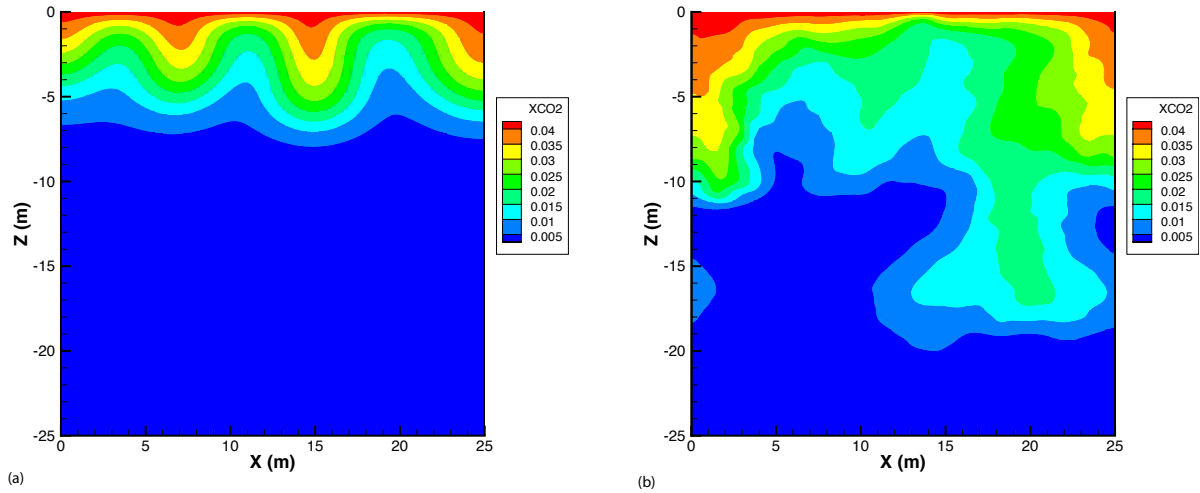
Figure 4.1: Dissolved mass fraction profile for (a) Homogenous model; (b) Heterogeneous model with horizontal barriers. Both examples at identical time. Figures taken from Green and Ennis-King (2009).

medium to represent vertical heterogeneity. An example of the effect of horizontal barriers on the development of convective fingering is presented in Figure 4.1. In this case, the homogenous model has an effective vertical permeability equal to the heterogeneous model. As Figure 4.1 demonstrates, the convective fingers have grown much faster for the heterogenous case compared to the homogeneous case. Through multiple realisations of similar cases, it was observed that convection began much earlier in this homogeneous setting than it did in a homogenous medium with identical effective permeabilities. If the characteristic length scale of the convection fingers at the onset of mixing were much smaller than the vertical separation between flow barriers, then the local vertical permeability was controlling parameter. This finding highlighted that heterogeneity on multiple length scales will be important as convection fingers grow, which has obvious implications for upscaling from high-resolution simulations to field-scale simulations. Similar observations are made by Lindeberg and Wessel-Berg (2011) for both regularly positioned and randomly distributed horizontal barriers.

Elenius and Gasda (2012) used a regular distribution of horizontal flow barriers to examine their influence on the dissolution rate of CO_2. By considering models with barriers of various lengths, Elenius and Gasda (2012) observed that the presence of barriers reduces the long-term stable mass flux in comparison to the case with no barriers, with an exponential decrease with increasing barrier length. Furthermore, Elenius and Gasda (2012) noted that as the barrier length was increased, the temporal growth in the vertical extent of the fingers decreased markedly.

A detailed numerical study of the influence the degree of spatial heterogeneity in permeability has on the character of density-driven dissolution rate of CO_2 in saline aquifers was presented by Farajzadeh et al. (2011). Using a spectral method to generate multiple realisations of permeability heterogeneity of various degree with the same high Rayleigh number, they observed three marked regimes characterised by the Dykstra-Parson coefficient, a measure of the extent of the heterogeneity. For small values of the Dykstra-Parsons coefficient, corresponding to a weakly heterogeneous permeability field, fingering analogous to the homogeneous case was observed, and this regime was termed the heterogeneous fingering regime, see Figure 4.2(b). In comparison to the homogeneous case, however, the amount of CO_2 dissolved in the heterogeneous case was found to be greater in most instances.

For medium values of the Dykstra-Parsons coefficient, representative of a moderate degree of heterogeneity, significant flux through some pathways of relatively higher local permeability was observed in most cases. This resulted in plumes dominated by the distribution of permeability. As a result, Fara-
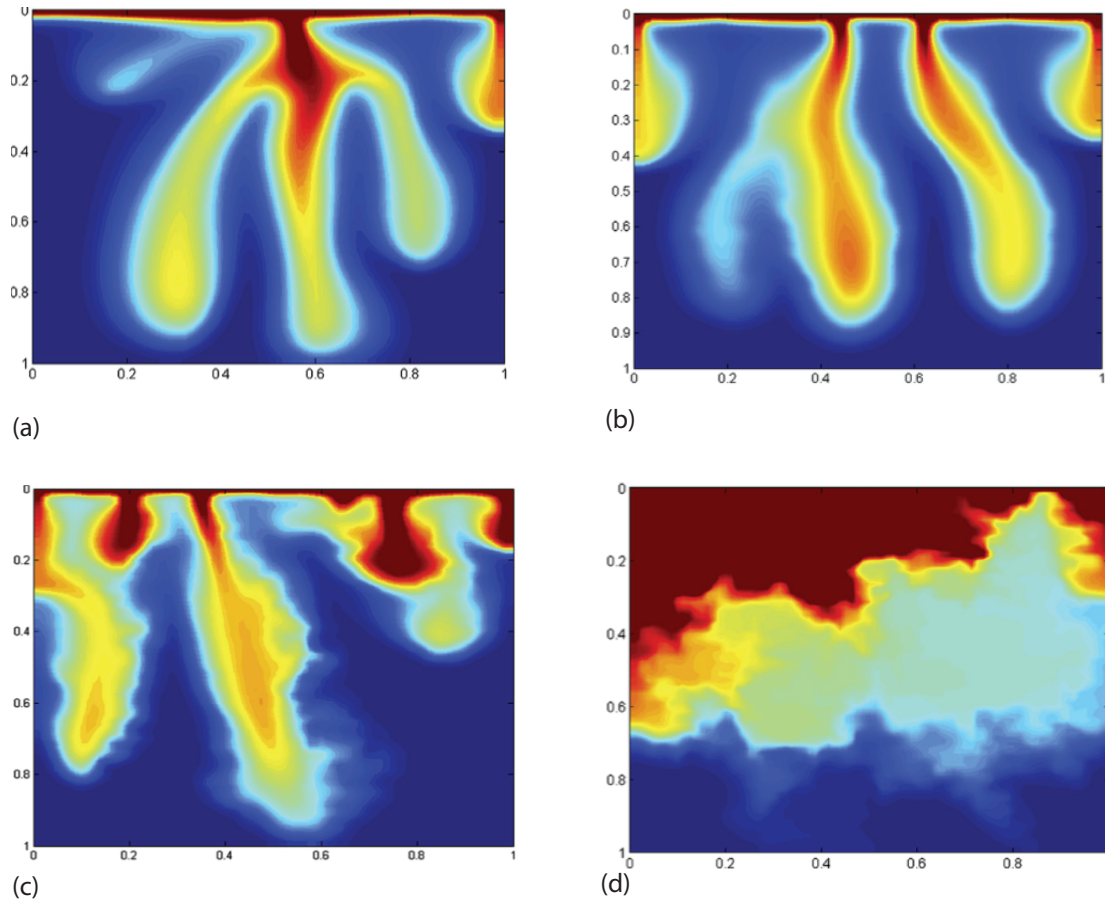
Figure 4.2: The heterogenous regimes identified by Farajzadeh et al. (2011). (a) Homogenous fingering; (b) Heterogeneous fingering; (c) Heterogenous channeling; (d) Heterogeneous dispersion. All examples at similar time. Figures taken from Farajzadeh et al. (2011).

jzadeh et al. (2011) termed this the channeling regime, see Figure 4.2(c) for an example. As for the heterogeneous fingering regime, the dissolution rate was typically greater than for the homogenous case.

Finally, for large Dykstra-Parsons coefficients, where heterogeneity is significant, the dissolution rate increased as the square root of time, suggesting that this regime could be adequately represented by a purely dispersive model with an appropriate diffusion coefficient. No fingering was observed, see Figure 4.2(d) for an example of the heterogeneous dispersive regime.

The work of Farajzadeh et al. (2011) was extended by Ranganathan et al. (2012) to study the effect of the Rayleigh number on the characteristic of density-driven dissolution of CO_2 in saline aquifers. Using a Sequential Gaussian Simulation method to construct heterogeneous permeability fields, they also observed three possible characteristic regimes from plots of the vertical mixing length (an arbitrary length defined by the authors as the vertical distance from the top boundary to the location where the concentration of CO_2 is 10% of its solubility) versus time. Depending on the value of Rayleigh number, the mass transfer of CO_2 is either dominated by diffusion, convective mixing, or features a mixing length growth slower than convection but nearly equal to the diffusive case. However, when the degree of permeability variation is significant, no diffusion-dominated regime is observed, and only two characteristic regimes are possible.

As expected, large-scale permeability heterogeneity can have a significant impact on the onset, rate

and characteristic behaviour of convective mixing of CO_2 in saline aquifers. The effects of small-scale heterogeneity, such as that associated with the spatial variation of the pore size distribution, has also been observed to effect the rate of dissolution. Aggelopoulos and Tsakiroglou (2012) presented experimental and numerical results of CO_2 dissolution in columns packed with granular porous media which suggested that while the dissolution rate in this idealised model is relatively unaffected by permeability variation due to the porosity heterogeneity, failing to account for the variation in hydrodynamic dispersion due to the porosity heterogeneity can lead to large discrepancies. It should be noted that the permeability variation considered in this study is small, and that larger permeability heterogeneity may lead to more significant changes to the dissolution rate.

5 Geochemistry

Another complicating factor that has not received a great deal of attention in the scientific literature is the role of geochemical reactions between the CO_2 and minerals present in the formation during sequestration. While slow reactions with typical minerals such as calcium present in the reservoir can take hundreds to thousands of years to precipitate a significant fraction of the injected CO_2, reactions with common carbonate minerals such as calcite can occur much faster and influence the onset of convective mixing in the short term.

Ennis-King and Paterson (2007) presented a theoretical and numerical study of the role of geochemistry on the onset and rate of convective mixing of CO_2. If chemical reaction were sufficiently slow, convective mixing could occur as if no reactions were occurring, and the only role geochemical reactions play is in the long-term mineralisation of CO_2. However, when fast acting reactions were considered, significant coupling between the reactions and convective mixing could be expected. First, the reaction could alter the density of the fluid due to changes in solute concentration or even temperature (either exothermic or endothermic). Secondly, reactions between the CO_2 and minerals in the reservoir rock may result in local variations to porosity and permeability. Ennis-King and Paterson (2007) demonstrated using a simple analytical model with a single mineral present that fast acting chemical reactions can lead to significant increases in the critical time for the onset of convective mixing. Including the effects of geochemical reactions, the critical time could be up to an order of magnitude greater than for the case with no reactions present. However, the wavelength of perturbations remained relatively unchanged.

This effect was considered in detail by Andres and Cardoso (2011), who showed that the density instability with fast chemical reactions was determined solely by the dimensionless parameter

$$\frac{Da}{Ra^2} = \frac{\phi \mu^2 k_r A D}{(k \Delta \rho g)^2} , \tag{5.1}$$

where Da is the dimensionless Damköhler number, which relates the reaction time to the flow transport time, k_r is the kinetic rate constant, and A is the area per unit volume of mineral. For $Da/Ra^2 \lesssim 0.002$, convection can occur, with a critical time to onset that grows linearly with increasing Da/Ra^2. This indicates that as the reactions occur faster (increasing Da at constant Ra), the critical time for the onset of convection is delayed, as observed by Ennis-King and Paterson (2007). For $Da/Ra^2 > 0.002$, chemical reactions are so rapid as to stabilise the diffusive layer at the CO_2-brine interface, and no convection is possible (Andres and Cardoso, 2011). However, these findings are for the simplified case where reactions continue indefinitely, and it is unclear how these results would be modified when reactions are limited by the finite amount of reactants.

Ghesmat et al. (2011b) presented a linear stability analysis of the effect of geochemical reactions on the onset of convective mixing, and confirmed that fast reactions typically stabilise the diffusive layer thus delaying the onset of convection by reducing the density contrast. Interestingly, the rate of trapped CO_2 was shown to increase in these cases, with mineralisation of CO_2 from the dissolved
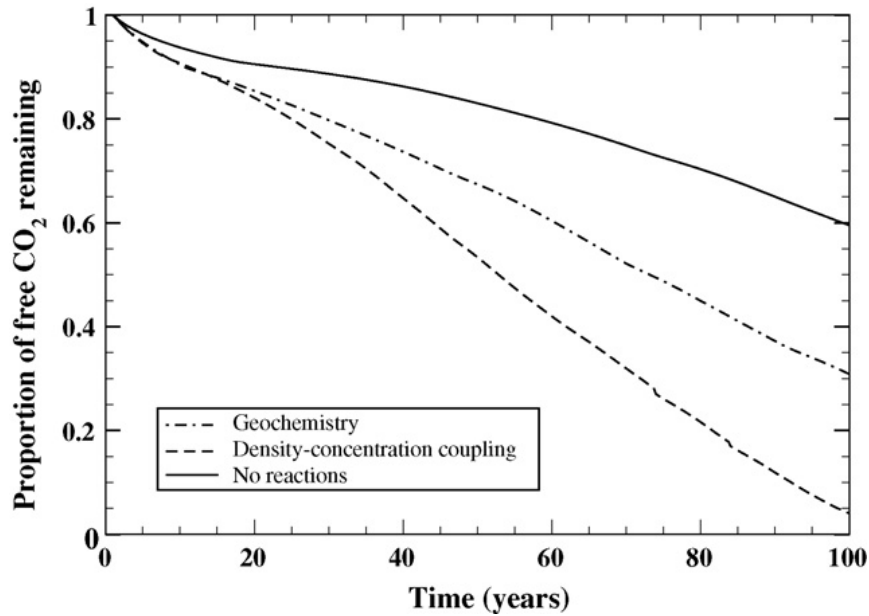
Figure 5.1: Proportion of mobile CO_2 dissolved due to convection for no reactions (solid line); geochemistry included (dotted-dashed line); coupling of ions to fluid density (dashed line). Figures taken from Ennis-King and Paterson (2007).

phase occurring at a rate faster than the decrease in convective mixing resulting from the reduced mass of dissolved CO_2.

Numerical simulations showed that including the effects of geochemical reactions could result in a significantly increased dissolution rate (Ennis-King and Paterson, 2007), see Figure 5.1. For instance, including reactions led to an increase of approximately 30% in the proportion of dissolved CO_2 after 100 years, even neglecting the effect on fluid density of the ionic concentration. When the contribution to the fluid density due to local ion concentration is included in the simulation, the dissolution rate increases further, with an additional 25% of the total CO_2 dissolved, see Figure 5.1.

In the cases considered by Ennis-King and Paterson (2007), local permeability decreases due to the presence of geochemical reactions was small, and insufficient to impede or inhibit convective mixing. However, it is feasible that some cases of practical interest may feature mineralogy that will enable reactions that will retard convection. Site specific simulations with accurate representations of the mineralogy will therefore be important in obtaining robust predictions.

One of the key findings of Ennis-King and Paterson (2007) that has not received a great deal of attention is that the increase in fluid density due to ion concentration can be of the same order of magnitude as the density increase due to dissolved CO_2. This effect can therefore be an important process in the onset and rate of convective mixing, as confirmed in the sensitivity analysis of Zhang et al. (2011). If this effect is neglected, predictions of the onset time and dissolution rates of convective mixing may vary significantly from their actual values.

6   Applications to field-scale modelling

Thus far, most of the research into convective mixing of CO_2 in a saline aquifer has been concerned with examining simple problems that are analytically tractable, such as estimating the critical time for the onset of convective mixing in a horizontal homogenous reservoir, or with fine-scale simulations

with computational domains of the order of metres in width. This is in contrast with field-scale simulations of CO_2 storage, which commonly feature individual grid blocks with dimensions at least one order of magnitude and sometimes two orders of magnitude greater than the total dimensions of these fine-scale models. Consequently, there is a disconnect in length scales between the results concerning convective mixing of CO_2 in saline aquifers currently available in the scientific literature, and the numerical simulations of a practical storage project.

The use of large grid blocks in these studies is necessitated by limits on the available computational power, and the common requirement to perform simulations on a suite of possible geological realisations to mitigate the uncertainty in many important parameters. However, these large grid blocks inhibit the onset of convection within the numerical simulation, and hence underestimate the rate of dissolution. Indeed, when considering the critical wavelength for convective fingers which could be on the centimetre scale (see Table 3.2, it is obvious that grid blocks of lateral dimensions that are several orders of magnitude greater than this will be unable to accurately capture the fingering process.

Comparatively few studies attempting to incorporate fine-scale convective mixing processes into field-scale simulations have been published. Pruess and Nordbotten (2011) included the enhanced dissolution as a result of sub-grid scale convective mixing in a large-scale simulation by way of a rudimentary sink term applied to the region in the uppermost row of grid blocks containing mobile phase CO_2. For the reservoir conditions of the problem considered, the onset time of convective mixing was estimated to be insignificant compared to the total simulation time, and as such, this process was assumed to take place instantaneously.

For a gently sloping reservoir, Pruess and Nordbotten (2011) found that increasing the dissolution rate in this fashion led to a CO_2 plume that was thinner as it migrated updip, while reducing the updip flux. Interestingly, the speed of the plume was unaffected by the inclusion of the sink terms.

Gasda et al. (2011) and Gasda et al. (2012) include the subgrid convection of CO_2 in a vertical equilibrium formulation (Gasda et al., 2009) using an upscaled representation of the dissolution and convection processes. Like Pruess and Nordbotten (2011), they assume that the convective mixing process begins instantaneously, and that the dissolution rate is linear for all times when gas phase CO_2 is present. Applying this model to some test problems, it was observed that including the enhanced dissolution due to convection could significantly reduce the updip distance travelled by the plume of CO_2, and hence reducing the total time in which the plume is migrating.

Mykkeltvedt and Nordbotten (2012) applied this vertical equilibrium approach to estimate the rate of convective mixing in the Utsira formation at the Sliepner field. This process results in a predicted dissolution rate due to convective mixing of 15 kg m^{-2} y^{-1}, which is comparable to measured estimates. Mykkeltvedt and Nordbotten (2012) note that this relatively high rate of dissolution cannot be explained without including the convective mixing process, suggesting that enhanced dissolution due to convective mixing can be important even during the injection process.

7 Future directions

It is clear that the disparate length scales at which convective mixing occurs and the size of the grid blocks used in field-scale simulations is a fundamental limitation on the accuracy of numerical simulations of CO_2 storage in saline aquifers. Due to the importance of convective mixing on the rate of dissolution, and hence the secure storage of CO_2, mechanisms for incorporating the enhanced dissolution rate due to convection are necessary for reliable numerical predictions.

Pruess and Nordbotten (2011) presented a simplistic implementation of the subgrid scale convection for a simple test problem using sink terms in the uppermost row of the regular simulation grid, while Gasda et al. (2011) have incorporated the steady long-term flux into a vertical equilibrium model.

In order to advance the inclusion of the fine-scale convective mixing process in field-scale simulations, further research into the dependence of the steady mass flux once convection has been established on parameters controlling the heterogeneity is necessary. The enhanced dissolution due to the convection may then be incorporated into field-scale simulations in a dynamic fashion, possibly through effective fluid or reservoir parameters, in a similar fashion to the usual permeability upscaling commonly employed in practice.

This will be important for numerical modelling of CO_2 storage in the Precipice Sandstone, where dissolution will play an important role in the long-term storage. To this end, this research project will study the long-term convective mass flux of CO_2 in heterogeneous reservoirs, first using a simple model of heterogeneity consisting of large lateral flow barriers as used by Green and Ennis-King (2009). Heterogeneity specific to the Precipice Sandstone can then be incorporated using results derived from the available log data. The role of geochemistry appropriate to the Precipice Sandstone on the long-term convective flux will also be examined. Following this, means to incorporate the fine-scale convective mixing results into field-scale simulations will be examined through inclusion of sub-grid scale methods into existing available software.

References

Aggelopoulos, C.A., Tsakiroglou, C.D., 2012. Effects of micro-heterogeneity and hydrodynamic dispersion on the dissolution rate of carbon dioxide in water-saturated porous media. Int. J. Greenh. Gas Con. 10, 341–350.

Andres, J.T.H., Cardoso, S.S.S., 2011. Onset of convection in a porous medium in the presence of chemical reaction. Physical Review E 83, 046312.

Bachu, S., Gunther, W.D., Perkins, E.H., 1994. Aquifer disposal of CO_2: hydrodynamic and mineral trapping. Energy Conserv. Mgmt. 35, 269–279.

Backhaus, S., Turitsyn, K., Ecke, R., 2011. Convective instability and mass transport of diffusion layers in a Hele-Shaw geometry. Physical Review Letters 106, 104501.

Bear, J., 1972. Dynamics of fluids in porous media. Dover Publications, New York.

Chen, C., Zhang, D., 2010. Pore-scale simulation of density-driven convection in fractured porous media during geological CO_2 sequestration. Water Resour. Res. 46, W11527.

Cinar, Y., Riaz, A., Tchelepi, H., 2007. Experimental study of CO_2 injection into saline formations, in: SPE Annual Technical Conference and Exhibition.

Duoxing, Y., Rongshu, Z., Deliang, Z., 2011. Numerical simulation of convective stability of the short-term storage of CO_2 in saline aquifers. Int. J. Greenh. Gas Con. 5.

Elenius, M.T., 2011. Convective mixing in geological carbon storage. Ph.D. thesis.

Elenius, M.T., Gasda, S.E., 2012. Impact of tight horizontal layers on dissolution trapping in geological carbon storage, in: XIX International Conference on Water Resources.

Elenius, M.T., Johannsen, K., 2012. On the time scales of nonlinear instability in miscible displacement porous media flow. Comp. Geosci. .

Ennis-King, J.P., Gibson-Poole, C.M., Lang, S.C., Paterson, L., 2002. Long-term numerical simulation of geological storage of CO_2 in the Petrel Sub-Basin, North West Australia. Proceedings of the Sixth International Conference on Greenhouse Gas Control Technologies , 1–6.

Ennis-King, J.P., Paterson, L., 2003. Role of convective mixing in the long-term storage of carbon dioxide in deep saline formations, in: SPE Annual Technical Conference and Exhibition, Denver, 5-8 October.

Ennis-King, J.P., Paterson, L., 2005. Role of convective mixing in the long-term storage of carbon dioxide in deep saline formations. SPE J. , 349–356.

Ennis-King, J.P., Paterson, L., 2007. Coupling of geochemical reactions and convective mixing in the long-term geological storage of carbon dioxide. Int. J. Greenh. Gas Con. 1, 86–93.

Ennis-King, J.P., Preston, I., Paterson, L., 2005. Onset of convection in anisotropic porous media subject to a rapid change in boundary conditions. Phys. Fluids 17, 084107.

Farajzadeh, R., Ranganathan, P., Zitha, P.L.J., Bruining, J., 2011. The effect of heterogeneity on the character of density-driven natural convection of CO_2 overlying a brine layer. Advances in Water Resources 34, 327–339.

Farajzadeh, R., Salimi, H., Zitha, P.L.J., Bruining, H., 2007. Numerical simulation of density-driven natural convection in porous media with application for CO_2 injection projects. Int. J. Heat Mass Tran. 50, 5054–5064.

Farajzadeh, R., Zitha, P.L.J., Bruining, H., 2009. Enhanced mass transfer of CO_2 into water: Eexperiment and modelling, in: SPE EUROPEC/EAGE Annual Conference and Exhibition, Amsterdam, The Netherlands, 8-11 June.

Gasda, S.E., Nordbotten, J.M., Celia, M.A., 2009. Vertical equilibrium with sub-scale analytical methods for geological CO_2 sequestration. Comp. Geosci. 13, 435–450.

Gasda, S.E., Nordbotten, J.M., Celia, M.A., 2011. Vertically averaged approaches for CO_2 migration with solubility trapping. Water Resour. Res. 47, W05528.

Gasda, S.E., Nordbotten, J.M., Celia, M.A., 2012. Application of simplified models to CO_2 migration and immobilization in large-scale geological systems. Int. J. Greenh. Gas Con. 9, 72–84.

Ghesmat, K., Hassanzadeh, H., Abedi, J., 2011a. The effect of anisotropic dispersion on the convective mixing in long-term CO_2 storage in saline aquifers. AIChE Journal 57, 561–570.

Ghesmat, K., Hassanzadeh, H., Abedi, J., 2011b. The impact of geochemistry on convective mixing in a gravitationally unstable diffusive boundary layer in porous media: CO_2 storage in saline aquifers. J. Fluid Mech. 673, 480–512.

Green, C.P., Ennis-King, J.P., 2009. Effect of vertical heterogeneity on long-term migration of CO_2 in saline formations. Transp. Porous Med. 82, 31–47.

Green, C.P., Ennis-King, J.P., 2010. Vertical permeability distribution of reservoirs with impermeable barriers. Transp. Porous Med 83, 525–539.

Green, C.P., Ennis-King, J.P., 2012. Spatial grid correction for short-term numerical simulation results of carbon dioxide dissolution in saline aquifers. Comp. Geosci. 16, 1153–1161.

Hassanzadeh, H., Pooladi-Darvish, M., Keith, D.W., 2005. Modelling of convective mixing in CO_2 storage. J. Can. Petrol Technol. 44, 43–51.

Hassanzadeh, H., Pooladi-Darvish, M., Keith, D.W., 2006. Stability of a fluid in a horizontal saturated porous layer: effect of non-linear concentration profile, initial, and boundary conditions. Transp. Porous Med. 65, 193–211.

Hassanzadeh, H., Pooladi-Darvish, M., Keith, D.W., 2007. Scaling behavior of convective mixing, with application to geological storage of CO_2. AIChE Journal 53, 1121–1131.

Hassanzadeh, H., Pooladi-Darvish, M., Keith, D.W., 2009. The effect of natural flow of aquifers and associated dispersion on the onset of buoyancy-driven convection in a saturated porous medium. AIChE Journal 55, 475–485.

Hesse, M.A., Riaz, A., Tchelepi, H.A., 2006. Resolving density fingering during CO_2 sequestration: a challenge for reservoir, in: Proceedings, CO2SC Symposium, pp. 1–4.

Hidalgo, J.J., Carrera, J., 2009. Effect of dispersion on the onset of convection during CO_2 sequestration. J. Fluid Mech. 640, 441–452.

Hodgkinson, J., Grigorescu, M., 2012. Background research for selection of potential geostorage targets—case studies from the Surat Basin, Queensland. Australian Journal of Earth Sciences , 1–19.

Hong, J.S., Kim, M.C., 2008. Effect of anisotropy of porous media on the onset of buoyancy-driven convection. Transp. Porous Med. 72, 241–253.

Jahangiri, H.R., Zhang, D., 2011. Effect of spatial heterogeneity on plume distribution and dilution during CO_2 sequestration. Int. J. Greenh. Gas Con. 5, 281–293.

Javaheri, M., Abedi, J., Hassanzadeh, H., 2010. Linear stability analysis of double-diffusive convection in porous media, with application to geological storage of CO_2. Transp. Porous Med. 84, 441–456.

Javaheri, M., Abedi, J., Hassanzadeh, H., 2009. Onset of convection in CO_2 sequestration in deep inclined saline aquifers, in: J. Can. Petrol. Technol., pp. 22–27.

Kihm, J.H., Kim, J.M., Wang, S., Xu, T., 2012. Hydrogeochemical numerical simulation of impacts of mineralogical compositions and convective fluid flow on trapping mechanisms and efficiency of carbon dioxide injected into deep saline sandstone aquifers. Journal of Geophysical Research 117, B06204.

Kneafsey, T.J., Pruess, K., 2010. Laboratory flow experiments for visualizing carbon dioxide-induced, density-driven brine convection. Transp. Porous Med. 82, 123–139.

Lindeberg, E., Bergmo, P.E.S., 2003. The long-term fate of CO_2 injected into an aquifer. Greenhouse Gas Control Technologies 1, 489–494.

Lindeberg, E., Wessel-Berg, D., 1997. Vertical convection in an aquifer column under a gas cap of CO_2, in: Energy Convers. Manag., pp. S229–S234.

Lindeberg, E., Wessel-Berg, D., 2011. Upscaling studies of diffusion induced convection in homogeneous and heterogeneous aquifers. Energy Proc. 4, 39273934.

Lu, C., Lichtner, P., 2007. High resolution numerical investigation on the effect of convective instability on long term CO_2 storage in saline aquifers. J. Phys. Conference Series 78, 1742–6596.

MacMinn, C.W., Neufeld, J.A., Hesse, M.A., Huppert, H.E., 2012. Spreading and convective dissolution of carbon dioxide in vertically confined, horizontal aquifers. Water Resour. Res. 48, W11516.

Macminn, C.W., Szulczewski, M.L., Juanes, R., 2011. CO_2 migration in saline aquifers. Part 2. Capillary and solubility trapping. J. Fluid Mech. 688, 321–351.

van der Meer, L.G.H., 1992. Investigations regarding the storage of carbon dioxide in aquifers in the Netherlands. Energy Conserv. Mgmt. 33, 611–618.

Moghaddam, R.N., Rostami, B., Pourafshary, P., Fallahzadeh, Y., 2012. Quantification of density-driven natural convection for dissolution mechanism in CO_2 sequestration. Transp. Porous Med. 92, 439–456.

Mykkeltvedt, T.S., Nordbotten, J.M., 2012. Estimating effective rates of convective mixing from commercial-scale injection. Environ. Earth Sci. .

Neufeld, J.A., Hesse, M.A., Riaz, A., Hallworth, M.A., Tchelepi, H.A., Huppert, H.E., 2010. Convective dissolution of carbon dioxide in saline aquifers. Geophys. Res. Lett. 37, L22404.

Nield, D.A., Kuznetsov, A.V., 2007. The effects of combined horizontal and vertical heterogeneity and anisotropy on the onset of convection in a porous medium. Int. J. Thermal Sci. 46, 1211–1218.

Nield, D.A., Simmons, C.T., 2006. A discussion on the effect of heterogeneity on the onset of convection in a porous medium. Transp. Porous Med. 68, 413–421.

Nield, D.A., Simmons, C.T., 2007. A discussion on the effect of heterogeneity on the onset of convection in a porous medium. Transp. Porous Med. 68, 413–421.

Pau, G.S.H., Bell, J.B., Pruess, K., Almgren, A.S., Lijewski, M.J., Zhang, K., 2010. High-resolution simulation and characterization of density-driven flow in CO_2 storage in saline aquifers. Advances in Water Resources 33, 443–455.

Prasad, A., Simmons, C., 2003. Unstable density-driven flow in heterogeneous porous media: A stochastic study of the Elder[1967b] "short heater" problem. Water Resour. Res. 39, 1007.

Pruess, K., Nordbotten, J.M., 2011. Numerical simulation studies of the long-term evolution of a CO_2 plume in a saline aquifer with a sloping caprock. Transp. Porous Med. 90, 135–151.

Pruess, K., Nordbotten, J.M., Zhang, K., 2009. Numerical simulation studies of the long-term evolution of a CO_2 plume under a sloping caprock. Proceedings, TOUGH Symposium 2009 , 1–7.

Pruess, K., Zhang, K., 2008. Numerical modeling studies of the dissolution-diffusion-convection process during CO_2 storage in saline aquifers. Lawrence Berkeley National Laboratory .

Ranganathan, P., Farajzadeh, R., Bruining, H., Zitha, P.L.J., 2012. Numerical simulation of natural convection in heterogeneous porous media for CO_2 geological storage. Transp. Porous Med. 95, 25–54.

Rees, D.A.S., Selim, A., Ennis-King, J.P., 2008. The instability of unsteady boundary layers in porous media, in: Vadasz, P. (Ed.), Emerging topics in heat and mass transfer in porous media. Springer, Netherlands.

Riaz, A., Hesse, M., Tchelepi, H.A., Orr, F.M., 2006. Onset of convection in a gravitationally unstable diffusive boundary layer in porous media. J. Fluid Mech. 548, 87–111.

Simmons, C.T., Nield, D.A., Kuznetsov, A.V., 2010. Effect of strong heterogeneity on the onset of convection in a porous medium: Importance of spatial dimensionality and geologic controls. Water Resour. Res. 46, W09539.

Slim, A.C., Ramakrishnan, T.S., 2010. Onset and cessation of time-dependent, dissolution-driven convection in porous media. Phys. Fluids 22, 124103.

Taheri, A., Wessel-Berg, D., Torsaeter, O., Soroush, M., 2012. The effects of anisotropy and heterogeneity on CO_2 dissolution in deep saline aquifers, in: Carbon Management Technology Conference. CMTC 151345.

Weir, G.J., White, S.P., Kissling, W.M., 1996. Reservoir storage and containment of greenhouse gases. Transp. Porous Med. 23, 37–60.

Woods, A.W., Espie, T., 2012. Controls on the dissolution of CO_2 plumes in structural traps in deep saline aquifers. Geophys. Res. Lett. 39, L08401.

Xu, X.F., Chen, S.Y., Zhang, D.X., 2006. Convective stability analysis of the long-term storage of carbon dioxide in deep saline aquifers. Advances in Water Resources 29, 397–407.

Yang, C.D., Gu, Y.G., 2006. Accelerated mass transfer of CO_2 in reservoir brine due to density-driven natural convection at high pressures and elevated temperatures. Ind. Eng. Chem. Res 45, 2430–2436.

Zhang, W., Li, Y., Omambia, A.N., 2011. Reactive transport modeling of effects of convective mixing on long-term CO_2 geological storage in deep saline formations. Int. J. Greenh. Gas Con. 5, 241–256.

CONTACT US

t 1300 363 400
  +61 3 9545 2176
e enquiries@csiro.au
w www.csiro.au

YOUR CSIRO

Australia is founding its future on science and innovation. Its national science agency, CSIRO, is a powerhouse of ideas, technologies and skills for building prosperity, growth, health and sustainability. It serves governments, industries, business and communities across the nation.

FOR FURTHER INFORMATION

CSIRO Earth Science & Resource Engineering
Chris Green
t +61 3 9545 8371
e chris.green@csiro.au
w www.csiro.au/cesre